

UVM ScholarWorks

The Entanglement Entropy and Quantum Sticking of a Cold Atom

Item Type	undergraduate thesis
Authors	Blake, Alice Dennett
Download date	2026-06-09 21:06:53
Item License	http://creativecommons.org/licenses/by-nc-nd/3.0/
Link to Item	https://hdl.handle.net/20.500.14849/5468

THE ENTANGLEMENT ENTROPY AND QUANTUM STICKING OF A COLD ATOM

A Thesis Presented

by

Alice Blake

to

The Faculty of the Honors College

of

The University of Vermont

In Fulfillment of the Requirements
For the Degree of Bachelor of Science with Honors
Specializing in Physics

May, 2023

Defense Date: May 5th, 2023

Honors Committee:

Dennis P. Clougherty, Ph.D., Advisor

Francois Dorais, Ph.D., Chairperson

Valeri Kotov, Ph.D.

ABSTRACT

An incident particle is drawn towards a neutral solid because of van der Waals attraction. When it collides, some of its energy goes to exciting vibrations of the solid. As a result of the collision, the particle could be adsorbed by the solid, or it could be scattered off the solid. The purpose of this thesis is to study the dynamics of a slow-moving, cold atom that collides with a two-dimensional solid, such as a hydrogen atom colliding with graphene. Using a time-dependent ansatz for the system wave function, we obtained coupled time-dependent equations that describe the possible outcomes of the collision. From these equations, the adsorption, or sticking, of the atom on a surface is studied. The numerical calculation shows for the case of N vibrational modes, the transition probability exhibits Rabi flopping. However, when the vibrons have a finite lifetime, the oscillations of the transition probability damp over time. From the calculations, the time dependent entanglement entropy (von Neumann entropy), $S(t)$, is subsequently studied. The entanglement entropy grows from zero to a local maximum and then falls to zero. At a later time, the calculations show “quantum revival” where the entanglement entropy again grows to a local maximum and subsequently collapses to zero. These results are discussed and interpreted in terms of the quantum sticking process.

CONTENTS

1	Introduction	1
1.1	History	4
1.2	Significance	5
2	The (N+1)-State Model	7
2.1	Multimode Rabi Model	10
2.2	Analytical Solution to the Single Mode Case	10
3	Numerical Solution	13
3.1	Parameters of Model	13
3.2	Single-mode Case	14
3.3	Multimode Case	17
3.4	Laplace Transform Method for the Multimode Solution	20
3.5	Fermi's Golden Rule	24
4	Density Matrix for the (N+1)-State Model	28
5	Entanglement Entropy	31
5.1	Single-Mode Case	33
5.2	Multimode Case	35
6	Conclusions and Future Work	40
	Bibliography	44

CHAPTER 1

INTRODUCTION

The process of atom adsorption is fundamental to science and technology. It is crucial in making materials, catalyzing chemical reactions, and changing surface properties of solids by coatings. Adsorption in the quantum regime is not fully understood. It involves the quantum dynamics of a many-body system. This provides the motivation to study simple models to acquire insights into the relevant physics. Entanglement entropy is a measure of how much two subsystems are quantum entangled. In the context of this thesis, entanglement entropy will be calculated using von Neumann entropy. Quantum sticking, also referred to as quantum adsorption, is when the incident atom transitions from the continuum to the bound state. Physically, this means it sticks to the surface. I will discuss a time-dependent ansatz for the system as a method to obtain a dynamical description of the particle as it collides with the surface. As this setup is somewhat abstract, the physical system that could correspond to my project would be a Hydrogen atom that collides and sticks to graphene, which is a single layer of carbon atoms.

One case of quantum sticking is the system of an atom colliding with a surface. For the purposes of this work, the system described is treated as a quantum dynamical system rather than a classical one because it has sufficiently low energy and involves

a system of mesoscopic size. While it is useful to consider classical analogs to the system, it is not useful for accurately describing the dynamics of the system.

It is important to note the difference between absorption and adsorption, as this thesis covers adsorption. In absorption, the atom would enter the pores of the surface. For adsorption, however, when the atom collides, it sticks to the surface without entering. Classically, adsorption can be observed when frost sticks the windshield of a car during the winter. Quantum mechanically, adsorption occurs when the atom transitions from a continuum state to the bound state localized on the surface.

Entanglement entropy was developed by John von Neumann after Lennard-Jones' paper on the interaction between two hydrogen atoms. In his 1955 book "Mathematical Foundations of Quantum Mechanics," von Neumann entropy is explained [1]. Von Neumann entropy is a mathematical way to quantify the quantum entanglement. It has a classical analog in Shannon entropy that is widely used in information theory.

The cold, slow-moving incident atom is drawn towards the surface to collide due to van der Waals attraction. This is the same force of attraction between two atoms that the Lennard-Jones paper explored. Thus, van der Waals interactions are fundamental to understanding the behavior of a cold, slow-moving atom close to a surface. First, to better understand this force, I will describe how it behaves for an atom-atom interaction, then I will describe its relevance to this thesis.

When two neutrally charged atoms are some distance, R , apart, there is a weak attraction between them, provided they are polarizable. So, despite each atom being neutral, each experiences a weak attraction. The attraction is dependent on the polarizability of the atom. The atom has electrons in orbitals that spin around the nucleus. As the electrons move around their respective nucleus, there are times when the electrons are unevenly distributed. This will cause moments when there are more electrons on one side than the other, causing one side of the atom to be negatively charged and the other side to be positively charged. At this time, the atom then

would be considered to be polarized and thus has an electric dipole moment [2].

The dipole moment in this atom occurs only briefly because the atom remains neutral. However, during the brief polarization, an attractive force between the two atoms arises. This brief attractive force from the temporary electric dipole is referred to as van der Waals force. Most often, van der Waals interaction is described using the potential. The van der Waals potential is written in equation 1.1 [3].

$$\Delta V = \frac{-\hbar}{8m^2\omega_0^3} \frac{e^2}{2\pi\epsilon_0} \frac{1}{R^6} \quad (1.1)$$

In equation 1.1, the distance between the two atoms is represented with R . It is important to note the potential is proportional to the inverse sixth power of the separation between the atoms [3]. This relation provides the foundation for describing the attraction potential between atoms. The same interactions occur between an atom and a two-dimensional surface, such as the setup I studied for this thesis. However, due to the geometry of the setup, the proportionality changes.

For the interaction between an incident atom and a surface, the van der Waals attraction is proportional to the inverse third power of the distance between the atom and the surface [4]. The atom-graphene van der Waals attraction has a different dependence than that of the atom-atom interaction because the geometry of the setup is different.

During the collision, energy goes into vibrating the graphene. The vibrational modes caused by the collision can be studied. The vibrations will damp because the edges of the surface are not physically able to be ideally clamped. The vibrations would also damp because the modes are not purely harmonic. Another cause of damping in vibrations is due to the imperfections in the graphene. Graphene is a two-dimensional layer of carbon, which has different isotopes. The disorder in the

distribution of carbon isotopes, along with vacancies in the graphene, contribute to vibrational damping. Mathematically, the damping can be included by allowing the vibrational frequencies to have a small imaginary term.

Another aspect of my research is to describe the time-dependent entanglement entropy $S(t)$ of the collision process. The density matrix, corresponding to the wave function considered was used to obtain an expression for the entanglement entropy $S(t)$. In Chapter 5, the time-dependent entanglement entropy is plotted for a variety of model parameters. These results give insight into the adsorption process.

1.1 HISTORY

Quantum sticking was first studied in the 1930s by John Edward Lennard-Jones and A. F. Devonshire. It was one of the first applications of the newly created quantum theory. Lennard-Jones published a paper in 1930 that explores the van der Waals attraction between two hydrogen atoms using perturbation theory [5]. Perturbation theory is a method for obtaining approximate solutions for an unsolvable Schrödinger equation. It involves separating the Hamiltonian into a piece that is solvable plus an additional term whose effects are hopefully small. In this work, the full time-dependent Schrödinger equation is solved numerically for a system wave function of a particular form. Thus, these results are non-perturbative.

Also in the 1930s, Dirac and Frenkel developed another method to approximately solve the Schrödinger equation that has become known as the Dirac-Frenkel time-dependent variational principle [6] [7]. This method can be used to justify the form of the wave function considered here. Furthermore, future work could vary the temperature, which would necessitate the use of the use of the Dirac-Frenkel time-dependent variational principle.

This thesis involves the dynamics of ultra-cold atoms, of which there are experi-

mental methods of verifying whether they behave in ways that match what we predict through theoretical work. Experimental research in the dynamics of ultra-cold atoms was revolutionized in the early 2000s when Bose-Einstein condensate was created in the laboratory by E. Cornell and C. Wieman [8]. Bose-Einstein condensate enabled experimental physicists to experimentally test quantum mechanical theory predictions about the dynamics of ultra-cold atoms. Bose-Einstein condensate was theoretically hypothesized years before it was experimentally created. When it finally was created, using optical molasses and evaporative physics, its creators were awarded a Nobel Prize [9]. Optical molasses involves slowing down atoms using lasers, while evaporative physics involves removing some atoms that are moving fast and have higher temperatures [10]. Using these methods, scientists cooled atoms to such a cold level they created a new state of matter we call Bose-Einstein condensate which allows us to test quantum mechanical theories.

1.2 SIGNIFICANCE

There are essential experimental applications relevant to understanding the mechanics of how cold atoms interact near surfaces. It can be useful for nano mechanical systems, such as precision mass sensors, resonators, and switches [11] [12]. The model used also has applications in quantum electrodynamics, where the description for vibrons can describe photons.

This thesis is within the realm of the emerging field of quantum information theory, which is a subfield of quantum mechanics that studies how quantum systems can be used for information storage and processing. This thesis makes progress towards answering some central questions behind quantum mechanics about how particles interact. For recent context in physics, my thesis expands upon the research of my thesis advisor, Dr. Dennis Clougherty, who derived the effective low energy model

for the quantum sticking of atoms on membranes [13] [14].

This thesis continues to study the dynamics of quantum sticking of atoms on membranes, but also expands the model by looking at the time dependence with the entanglement entropy. Through this work, the time-dependent probability and the behavior of the entanglement entropy for a system with a single vibrational mode and the multimode case were obtained numerically. These results are presented and interpreted in subsequent chapters.

CHAPTER 2

THE (N+1)-STATE MODEL

The Schrödinger equation is the foundation for quantum mechanics and is shown in Eq. (2.1) in bra-ket notation. This equation describes the behavior over time of the quantum state of the system and permits the prediction of the behavior of a quantum system. The wave function is Ψ and the Hamiltonian \hat{H} , which describes the energy of the system, is an operator.

$$i\hbar \frac{\partial}{\partial t} |\Psi\rangle = \hat{H} |\Psi\rangle \quad (2.1)$$

The Hamiltonian is the multimode Rabi model and is a simplified version of the model studied by Clougherty [13].

$$\hat{H} = E_c c^\dagger c - E_b b^\dagger b + \sum_{n=1}^N \hbar\omega_n a_n^\dagger a_n - g(c^\dagger b + b^\dagger c) \sum_n (a_n + a_n^\dagger) \quad (2.2)$$

The system wave function can be assumed to be approximated by the time-dependent ansatz given in Eq. (2.3)

$$|\Psi(t)\rangle = C(t)(|c\rangle \otimes |0\rangle) + \sum_{n=1}^N B_n(t)(|b\rangle \otimes |1_n\rangle) \quad (2.3)$$

As indicated by $|\Psi(t)\rangle$, while the solid is in the vibrational ground state, then the state space consists only of the atom in the $|c\rangle$ -state. When the atom has a quantum of vibration, it is said to have one vibron. The atom in the $|b\rangle$ -state with one vibron is present in the n^{th} mode.

The wave function, $|\Psi(t)\rangle$, is the solution to the time-dependent Schrödinger equation and can be expressed as a linear combination of the two possible states for a single vibrational mode. The coefficients of each wave function are promoted to time-dependent functions. These coefficients correspond to probability amplitudes, which informs the probability the atom is in a particular quantum state. The function $C(t)$ corresponds to the continuum state and the function $B(t)$ corresponds to the bound state. Further, the energy E_c corresponds to the atom energy when in the $|c\rangle$ -state and the energy $-E_B$ is the energy in the bound state. And so, the ansatz for the single mode case can be expressed in Eq. (2.4). States are products of the atom state with the vibrational state.

$$|\Psi(t)\rangle = C(t)(|c\rangle \otimes |0\rangle) + B(t)(|b\rangle \otimes |1\rangle) \quad (2.4)$$

Substitution of Eq. (2.4) into Eq. (2.1) yields a set of coupled, first-order ordinary differential equations (ODEs) for the atom amplitudes.

The case of a single vibrational mode ($N = 1$) with angular frequency ω , is described as follows:

$$i\frac{dC(t)}{dt} = \Omega_C C(t) - \alpha B(t) \quad (2.5)$$

$$i\frac{dB(t)}{dt} = \Omega_B B(t) - \alpha C(t) \quad (2.6)$$

where $\Omega_C = \frac{E_c}{\hbar}$, $\Omega_B = \frac{-E_b + \omega}{\hbar}$ and $\alpha = \frac{g}{\hbar}$.

I can solve Eqs. (2.5) and (2.6) analytically using methods of differential equations and numerically using Mathematica. The numerical solutions can be plotted to see the time dependence of the probability amplitudes $C(t)$ and $B(t)$. Subsequently, the solutions to Eqs. (2.5) and (2.6) are used to calculate the entanglement entropy. This same process can be applied to obtain solutions for the multimode case, when there is more than one vibrational mode ($N > 1$).

Eqs. (2.5) and (2.6) can be rewritten with two parameters instead of three by dividing both sides of each equation by Ω_C . The parameter Ω_C carries units of sec^{-1} . Thus, the parameters used throughout this research were rescaled by a factor of E_c/\hbar . The equations, rescaled to only have two parameters, that correspond to the single mode case are given in Eqs. (2.7) and (2.8). The new parameters correspond to dimensionless coupling (p) and a dimensionless frequency (w).

$$i\dot{C}(t) = C(t) - pB(t) \quad (2.7)$$

$$i\dot{B}(t) = wB(t) - pC(t) \quad (2.8)$$

2.1 MULTIMODE RABI MODEL

The previous results can be generalized to the case of $N > 1$. The following ODEs result:

$$i\hbar \frac{dC(t)}{dt} = E_c C(t) - g \sum_{n=1}^N B_n(t) \quad (2.9)$$

$$i\hbar \frac{dB_n(t)}{dt} = (-E_b + \hbar\omega_n) B_n - gC(t) \quad (2.10)$$

In Eqs. (2.9) and (2.10), E_c is the energy of the atom in the continuum, which can also be referred to as the gas phase. The energy E_b is the energy of the adsorbed atom to the solid. The model assumes that the vibrational frequencies are evenly spread by $\Delta\omega$. Thus, $\omega_n = \omega_0 + n\Delta\omega$, where $n = 1, 2, 3 \dots N$. The parameter g is a coupling constant that represents the interaction of the atom to the vibrations. To have resonance with the bounds state, it must hold true that $\frac{E_c + E_b}{\hbar} < \omega_0 + N\Delta\omega \equiv \omega_{max}$.

The solution to these equations will be discussed in Chapter 3.

2.2 ANALYTICAL SOLUTION TO THE SINGLE MODE CASE

Eqs. (2.7) and (2.8), the system of coupled differential equations that describe the single mode case, can be exactly solved using methods of ordinary differential equations. First, take the derivative of Eq. (2.7) to get $\ddot{C}(t)$. The result is shown below in Eq. (2.11).

$$i\ddot{C}(t) = \dot{C}(t) - p\dot{B}(t) \quad (2.11)$$

Now I can substitute in for $\dot{B}(t)$ from Eq. (2.8) and simplify. This gives Eq. (2.12).

$$i\ddot{C}(t) = \dot{C}(t) + iwpB(t) - ip^2C(t) \quad (2.12)$$

After making another substitution and simplifying, I have the equation below for the second derivative of $C(t)$.

$$i\ddot{C}(t) = (iw + i)\dot{C}(t) + (p^2 - w)C(t) \quad (2.13)$$

Eq. (2.13) is now uncoupled and in the form of a second order linear ordinary differential equation and can be solved. Due to its form, the solution will look like:

$$C(t) = k_1e^{s_1t} + k_2e^{s_2t} \quad (2.14)$$

where s_1 and s_2 are given below.

$$s_1 = \frac{i(1+w)}{2} + \frac{1}{2}\sqrt{(i+iw)^2 - 4(w-p^2)} \quad (2.15)$$

$$s_1 = \frac{i(1+w)}{2} - \frac{1}{2}\sqrt{(i+iw)^2 - 4(w-p^2)} \quad (2.16)$$

The values k_1 and k_2 are constants that could be found using the initial conditions. Also, now that we have $C(t)$, we also would like to know $B(t)$. However, the square modulus of $C(t)$ and $B(t)$ are more important than the expression for $C(t)$ itself since they represent probabilities of the quantum states. It is known that $|B(t)|^2 + |C(t)|^2 = 1$. And so, the simplest way to find $|B(t)|^2$ is to set $|B(t)|^2 = 1 - |C(t)|^2$.

$$|B(t)|^2 = 1 - |k_1 e^{s_1 t} + k_2 e^{s_2 t}|^2 \quad (2.17)$$

Using the initial conditions, I can solve for k_1 and k_2 . They are presented below, in terms of s_1 and s_2 .

$$k_1 = \frac{-i + s_2}{s_2 - s_1} \quad (2.18)$$

$$k_2 = 1 - \frac{-i + s_2}{s_2 - s_1} \quad (2.19)$$

From the analytical solution, we conclude the resonance condition is satisfied when $w = 1$. This is consistent with the definition of w and the condition $E_c + E_b = \hbar\omega_n$.

CHAPTER 3

NUMERICAL SOLUTION

Using a system wave function ansatz, we obtained Eqs. (2.7) and (2.8) to describe the possible outcomes of the collision. They can be solved to obtain solutions for $B_n(t)$ and for $C(t)$, which reveal the probability amplitudes. $|B(t)|^2$ versus time $|C(t)|^2$ versus time are plotted to reveal the complex dynamics of the adsorption process.

Within the description of the collision of the atom with a surface, I explored both the single-mode case and the multimode case. Mathematically, each new mode introduces another equation, $B_n(t)$ and the different modes have different frequencies, so the vibrational spectrum has N frequencies, between ω_0 and ω_{max} .

3.1 PARAMETERS OF MODEL

The energy of the incident atom is represented as E_C , which is representative of the atom in the continuum or the gas phase. When the atom collides with the surface, it transfers energy that goes to the vibrations of the surface. If the atom sticks, then it is trapped in a bound state. The bound state has a negative energy, E_b . The binding energy E_b is approximately 40 meV for atomic hydrogen on suspended graphene [15].

The equations are written using parameters p and w , where $p = \frac{g}{E_c}$ and $w =$

$\frac{-E_b + \hbar\omega}{E_c}$, so w is dependent on the frequency. For simplicity, p was kept at a constant 0.01 throughout the plots, which is small to be comparable to experimental conditions.

3.2 SINGLE-MODE CASE

Mathematica numerically solved Eqs. (2.7) and (2.8), subject to initial conditions $B(0) = 0$ and $C(0) = 1$. The result is a function, thus its solution can be represented graphically. $|B(t)|^2$ and $|C(t)|^2$ represent the probability amplitudes of the quantum states of the atom. For instance, when $|B(t)|^2$ is significantly greater than $|C(t)|^2$, then it is likely the atom is in the bound state, since $B(t)$ corresponds to the bound state and $C(t)$ corresponds to the continuum. As such, the initial conditions inform that the atom begins in the continuum state and has not yet collided with the surface, at time = 0.

First, I solved the equation of motion using real numbers for p and w . The plot of $|C(t)|^2$ versus time is shown in Fig. (3.1).

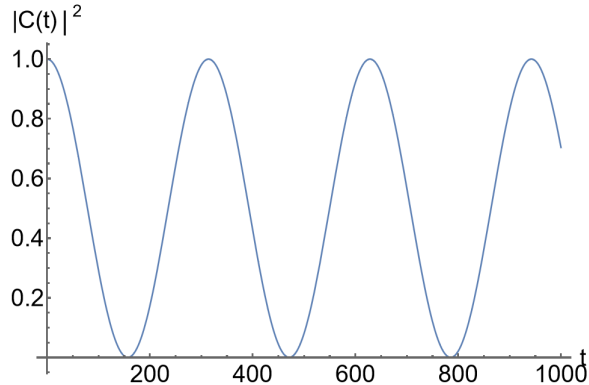


Figure 3.1: $|C(t)|^2$ versus time for single vibrational mode on-resonance using parameters $p = 0.01$, $w = 1$

In Fig. (3.1), with real parameters for p and w , there is no damping. The $w = 1$ parameter was used to satisfy the resonance condition and $p^2 \ll 1$ was used to make

contact with experimental conditions. The oscillations return to 1 at each maximum and 0 at each minimum. This behavior is referred to as Rabi flopping, which is when the atom oscillates between the $|c\rangle$ -state and the $|b\rangle$ -state [16]. At each maximum, the atom is in the continuum and at each minimum, the atom is in the bound state. The time, plotted on the x-axis, is not strictly in seconds since it has been multiplied by a scale factor to reduce the number of parameters. The vertical axis corresponds to the probability and it oscillates between 1 and 0. As the Rabi flopping pattern behavior continues forever, then the atom would not adsorb onto the membrane for the situation graphed in 3.1.

The period in Fig. (3.1) is given by $T = 100\pi$. This is recovered from the input parameter, $p = 0.01$. The frequency $2p$, which is known from the frequency expression that is found from the analytical solution to the equations of motion, $\sqrt{(w - 1)^2 + 4p^2}$. Since $w = 1$ was used, then the frequency simplifies to $2p$, and so when $p = 0.01$, then the frequency is 0.02. From the relationship $T = \frac{2\pi}{\omega}$, $T = 314$, which is exactly what is seen on Fig. (3.1).

Fig. (3.2) plots $|C(t)|^2$ versus time for an off-resonance case.

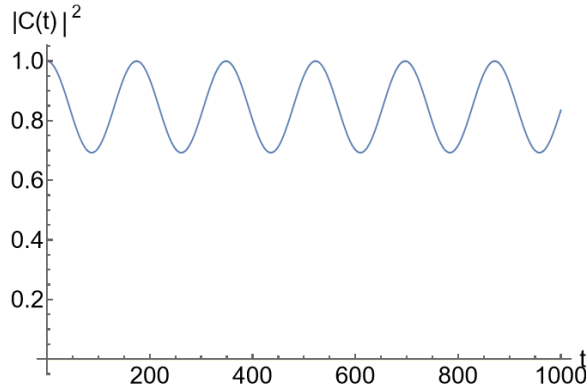


Figure 3.2: Plot of $|C(t)|^2$ versus time for $p = 0.01$ and $w = 0.97$.

When the parameters p and w are real, the plots for $|C(t)|^2$ versus time and $|C(t)|^2$ versus time oscillate without any damping. The atom oscillates between the

continuum and approximately 0.7 probability of being in the continuum, as is seen from the vertical axis minimum value. However, these non-damped oscillations do not correspond to a physical system.

In a real physical system of an incident Hydrogen atom colliding with graphene, it would be difficult to see the oscillatory behavior exhibited in Fig. (3.1). To see undamped oscillations, it would require a solid of small size so that only a few vibrational modes would exist. Vibrational energy loss would also need to be sufficiently low. For a real world situation, the oscillations would damp throughout time. When the atom collides with the surface, the energy is transferred into vibrations of the surface. One cause of vibrational energy loss is that it would not be possible to ideally clamp the edges of the surface. The vibrations would also damp because the modes are not purely harmonic and because of imperfections in the graphene. Graphene is a two-dimensional layer of carbon, which has different isotopes. The disorder in the distribution of carbon isotopes, along with vacancies in the graphene, contribute to damping. These defects are summarized in the imaginary part of the input parameter.

Since a system with damping would be more true to the real world, the vibrational frequencies are given a small imaginary part, which leads to damping.

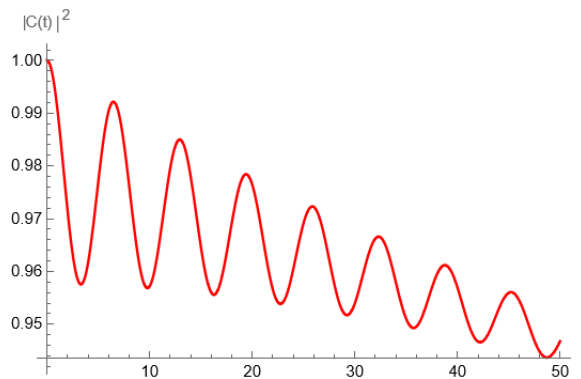


Figure 3.3: $|C(t)|^2$ versus time for single mode with parameters $p = 0.1$ and $w = -0.03i + 0.05$

As expected, the plot in Fig. (3.3) shows oscillations that damp with time. The

plot is for the off-resonance case.

Below is a plot of $|C(t)|^2$ versus time for when there is resonance and damping.

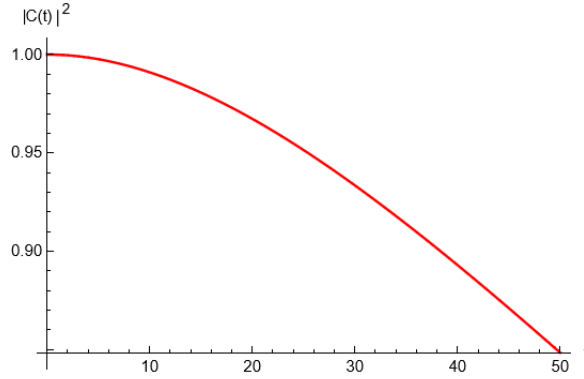


Figure 3.4: $|C(t)|^2$ versus time for single mode using parameters $p = 0.01$ and $w = 1 - 0.03i$

In Fig. (3.4), the probability amplitude of the atom in the continuum decreases.

The values of $|B(t)|^2$ and $|C(t)|^2$ represent probabilities and sum to zero for the idealized situation when there is no vibrational damping. However, as the vibrational frequencies are complex, they do not always sum to 1.

3.3 MULTIMODE CASE

For each mode added, the system gains an equation, $B_n(t)$. The coupled equations that describe the motion of the atom colliding with the membrane for the two mode case are written in Eqs. (3.1), (3.2), and (3.3). They are subject to the similar initial conditions as one mode, where $B_1(0) = 0$, $B_2(0) = 0$, and $C(0) = 1$. The addition of the mode also adds a term to Eq. (3.1).

$$i\dot{C}(t) = C(t) - p(B_1(t) + B_2(t)) \quad (3.1)$$

$$i\dot{B}_1(t) = w_1 B_1(t) - pC(t) \quad (3.2)$$

$$i\dot{B}_2(t) = w_2 B_2(t) - pC(t) \quad (3.3)$$

The same pattern follows for more modes, where an equation is added for each mode. The initial conditions of $B_n(0) = 0$ and $C(0) = 1$ are always satisfied. To go from the one mode case to the two mode case, I change the real part of w . As outlined in the parameters of the model, $w_n = \frac{-E_b + \hbar\omega}{E_c}$. As such, the dimensionless parameter, w_n is dependent on the vibrational frequency, ω_n . Eqs. (3.2) and (3.3) each carry a different value for the frequency. There is some initial frequency, ω_1 and some maximum frequency ω_N . The corresponding parameters w_n are the coefficients of B_n . The spacing between each frequency, $\Delta\omega$ must be equal. Thus, it follows that for each mode added, the frequency spacing decreases.

Below, in Fig. (3.5), I plotted both $|B_1(t)|^2$ versus time and $|B_2(t)|^2$ versus time.

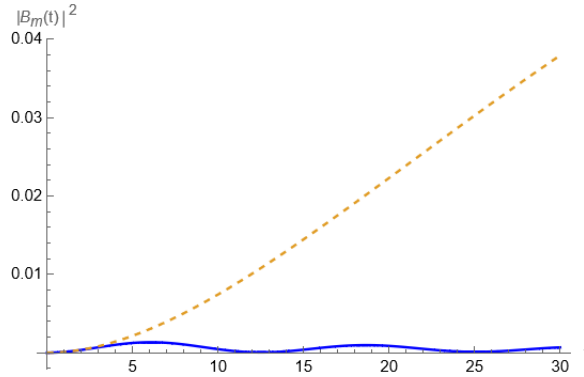


Figure 3.5: $B_1(t)$ versus time (blue) using $p = 0.1$, $w_1 = 0.05 - 0.03i$ and $B_2(t)$ versus time (Orange Dashed) using $p = 0.1$, $w_2 = 0.1 - 0.03i$, $N = 2$

The plot in Fig. (3.5) shows the plot of $|B_1(t)|^2$ versus time in the solid blue curve and the plot of $|B_2(t)|^2$ versus time in the dashed orange curve. Since each begins with the same initial conditions, the plots begin together, but diverge. The orange dashed curve, $|B_2(t)|^2$ has resonance with $|C(t)|^2$ and has a small imaginary part to

model the finite lifetime of the vibron. The blue curve, $|B_1(t)|^2$ is off-resonance with $|C(t)|^2$ and so it oscillates.

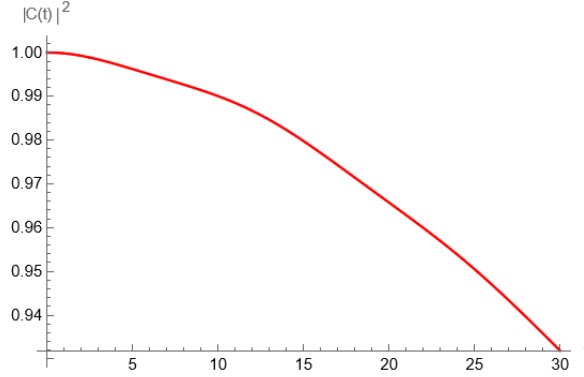


Figure 3.6: $|C(t)|^2$ versus Time for 2 Mode $p = 0.01$, $w_1 = 0.5 - 0.03i$, and $w_2 = 1 - 0.03i$

Fig. (3.6) plots $|C(t)|^2$ versus time for the same conditions as in Fig. (3.5). During this time period, the probability the particle is in the continuum state decreases.

After the two mode case, other multimode cases follow similarly. For each increasing mode, I generate a graph by adding an equation $B_k(t)$. For each mode, the frequency has the same minimum at some ω_1 and has the same maximum at some ω_N . The change in frequency, $\Delta\omega$, must be constant for all frequencies within a certain mode, N. Thus, for each mode added, $\Delta\omega$ will decrease. To demonstrate, I will plot all $|B_k(t)|^2$ for the 3 mode case in Fig. (3.7).

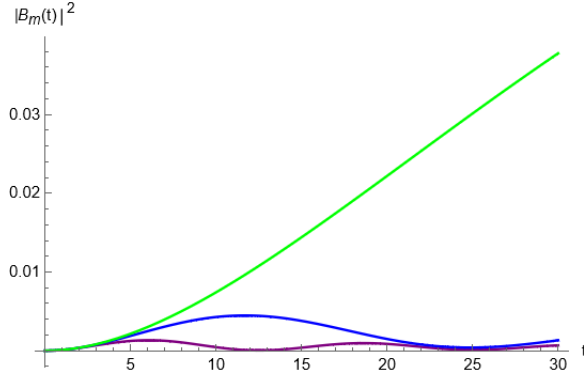


Figure 3.7: $|B(t)|^2$ versus time for 3 modes using parameters $p = 0.01$ and $w_1 = 0.5 - 0.03i$, $w_2 = 0.75 - 0.03i$, and $w_3 = 1 - 0.03i$

In Fig. (3.7), the frequencies are $w_1 = 0.05$, $w_2 = 0.075$, and $w_3 = 0.1$. So, the frequencies obey equal spacing and the frequency spacings are smaller than the frequency spacings in the $N = 2$ case. In Fig. (3.7), the green curve represents $|B_3(t)|^2$, the blue curve is $|B_2(t)|^2$, and the purple curve is $|B_1(t)|^2$. The green curve, $|B_3(t)|^2$ is on-resonance.

3.4 LAPLACE TRANSFORM METHOD FOR THE MULTIMODE SOLUTION

The generalized multimode equations of motion for the atom amplitudes, $C(t)$ and $B_n(t)$ can be reviewed below in Eqs. (3.4) and (3.5), as they were derived in section 2.1.

$$E_c C(t) - g \sum_n B_n(t) = i \frac{dC(t)}{dt} \tag{3.4}$$

$$(-E_b + \omega_n) B_n(t) - g C(t) = i \frac{dB_n(t)}{dt} \tag{3.5}$$

The Laplace transform method is a method to solve differential equations that uses an integral with respect to time to transform a time-dependent equation to the complex s-plane. The Laplace transform is defined for $C(t)$ below:

$$\bar{C}(s) \equiv \int_0^{\infty} e^{-st} C(t) dt \quad (3.6)$$

The same relation follows for $B_n(t)$. Applying initial conditions $C(0) = 1$ and $B_n(0) = 0$ and taking the Laplace transforms of Eqs. (3.4) and (3.5) yields the equations below.

$$i(s\bar{C}(s) - 1) = -g \sum_n \bar{B}_n(s) + E_c \bar{C}(s) \quad (3.7)$$

$$is\bar{B}_n(s) = -(E_b - \omega_n)\bar{B}_n(s) - g\bar{C}(s) \quad (3.8)$$

Then, by isolating for $\bar{B}_n(s)$ in Eq. (3.8) and then substituting into Eq. (3.7), the equation below is obtained.

$$\bar{C}(s) = \frac{i}{is - g^2 \sum_{n=1}^N \frac{1}{is + E_b + E_c - \omega_0 - (n-1)\Delta\omega}} \quad (3.9)$$

Subsequently, the inverse Laplace transform returns $\bar{C}(s)$ to $C(t)$. The integral that defines the inverse Laplace transform is shown in Eq. (3.10).

$$C(t) = \frac{1}{2\pi i} \int_{-i\infty+\epsilon}^{i\infty+\epsilon} e^{st} \bar{C}(s) ds \quad (3.10)$$

The integrand has poles when the denominator of $\bar{C}(s)$ vanishes. The complex variable z can be defined as $z = is$. So, setting the denominator of $\bar{C}(s) \rightarrow 0$ can be written as $z - F(z) = 0$, where the function $F(z) \equiv g^2 \sum_{n=1}^N \frac{1}{z + (E_b - \omega_0 + \Delta\omega) - n\Delta\omega}$.

By the fundamental theorem of algebra, there will be $N+1$ poles. The pole locations can be estimated graphically by plotting $F(z)$ and finding where it intersects the line with slope 1. The poles will be spaced approximately as $\Delta\omega$, with a minimum pole at $-z_0 + \Delta\omega$ and a maximum pole at $-z_0 + N\Delta\omega$. Then, using the approximate location, the poles can be plotted on the complex s -plane and the inverse Laplace transform can be calculated using the Residue Theorem, analytically.

Estimating the integral yields an approximate expression for $C(t)$.

$$|C(t)|^2 \approx \frac{[\sin(\frac{N-1}{2}\Delta\omega t)]^2}{[\sin(\frac{\Delta\omega t}{2})]^2} e^{-\gamma t} \quad (3.11)$$

The result suggests that the true $|C(t)|^2$ is periodic and has peaks of high probability of the particle being in the continuum at $\frac{2\pi}{\Delta\omega}n$, which means the particle exhibits quantum revival. In what follows, we choose units where $\Delta\omega = 1$. Then the period is approximately 2π . The damping factor, $e^{-\alpha t}$ causes the maxima to decrease over time due to damping and will shift the poles to the left or right of the imaginary axis. This result is shown below, after being numerically evaluated using Mathematica.

Fig. (3.8) shows the plot from a numerical calculation of Eq. (3.10) when there is no damping. It models the probability amplitude of the continuum for when $g = 0.5$, $b = 5$, and there are 10 modes.

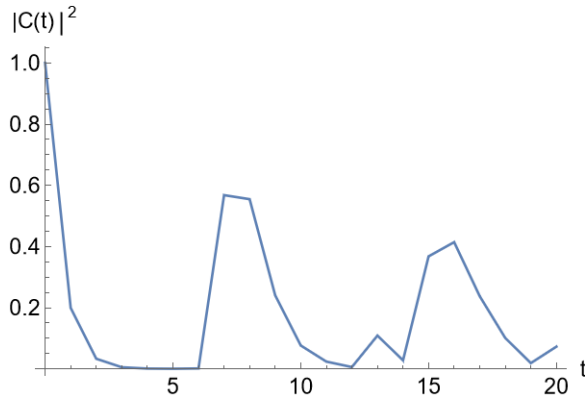


Figure 3.8: $C(t)$ versus time for 10 vibrational modes

As is consistent with the mathematical approximation for $|C(t)|^2$, the numerical plot is quasi-periodic at approximately 2π . The peaks decrease because the frequency spacing is not quite regular. When the vibrational frequencies become complex, then the probability amplitude shows more significantly damped oscillations.

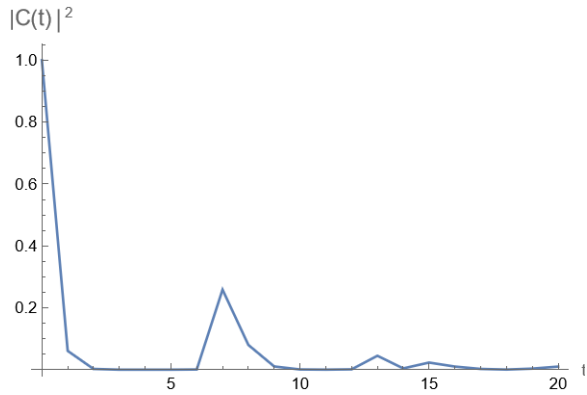


Figure 3.9: $C(t)$ versus time for 10 vibrational modes

Figure 3.9 plots the probability amplitude of the continuum state for when $b = 5 - i\frac{\pi}{6}$. As time passes, the probability of the atom being in the continuum decreases, with maxima at approximately $t_n = 2\pi n$.

3.5 FERMI'S GOLDEN RULE

Fermi's Golden Rule governs energy state transitions [3]. When a particle transitions from a discrete energy, E_i to E_f , it satisfies the resonance condition: $E_f = E_i + \hbar\omega_R$. In this context, E_i is the initial state, E_f is the final state, and ω_R is the resonant frequency. Fermi's Golden Rule is useful because it provides an equation to describe the transition rate with which the atom changes energy states [17]. Within my work, there is an atom that begins in the continuum and then moves towards a surface, due to van der Waals attraction, and if it sticks, then it transitions to a bound state. Whence, Fermi's Golden Rule can describe the transition probability per unit time that the atom drops energy states from the continuum to the bound state.

Mathematically, Fermi's Golden Rule can be expressed in Eq. (3.12) where it computes the adsorption rate, Γ_{GR} [17]. In the notation, $|i\rangle$ is when the atom is in the continuum and there are no vibrons. Meanwhile, $|f\rangle$ is when the atom is in the bound state and there is one phonon in the m^{th} mode.

$$\Gamma_{GR} = \frac{2\pi}{\hbar} |\langle f | H_1 | i \rangle|^2 \delta(E_f - E_i) \quad (3.12)$$

The matrix element $|\langle f | H_1 | i \rangle|^2$ is equivalent to g^2 , where g is the coupling strength, as first mentioned in section 3.2. The coupling strength is a measure of the strength of coupling of the system. It measures the efficiency with how the atom interacts with vibrational modes. The greater the coupling strength, the greater possibility the particle will give up energy to vibrational modes. It has dimensionality of energy. In most instances, the coupling strength would change with the mode. However, in the context of my work, the coupling strength is taken to be independent of the mode because graphene is two-dimensional [13]. Fermi's Golden Rule applies

only to the early time behavior of the decay [18].

A common application of Fermi's Golden Rule is used in the context of a particle initially being in a bound state, then getting bumped up an energy level and ending up in a final energy continuum [3]. The energy transition of starting in a bound state and moving into a continuum would require some additional energy. For the context of this work, an atom begins in the continuum and then ends in a bound state, if it is adsorbed.

Eq. (3.12) is the application to the single-mode case. To apply Fermi's Golden Rule to the multimode case and obtain the adsorption rate, we would sum over the modes. In the equation below, E_b is the energy of the bound state and is defined such that $E_b > 0$.

$$\Gamma_{GR} = \sum_N \frac{2\pi}{\hbar} g^2 \delta(\hbar\omega_N - E_c - E_b) \quad (3.13)$$

Eq. (3.13) can be simplified further by making the continuum approximation.

$$\Gamma_{GR} \approx \int_{\omega_0}^{\omega_N} D(\omega) d\omega \frac{2\pi}{\hbar} g^2 \delta(\omega\hbar - E_c - E_B) \quad (3.14)$$

Then, integrate over the frequencies from the initial frequency, ω_0 until a final frequency, ω_N , to obtain an equation for the adsorption rate. Invoke the scaling property of the delta function, which determines that $\delta(\omega\hbar - E_c - E_B) = \frac{1}{\hbar} \delta(\omega - \frac{E_c + E_B}{\hbar})$. And so, the equation below is the multimode adsorption rate.

$$\Gamma_{GR} = \frac{2\pi}{\hbar^2} g^2 D\left(\frac{E_c + E_B}{\hbar}\right) \quad (3.15)$$

The transition rate can be simplified using the assumptions $\hbar = 1$ and the density of states is 1 because there is one vibron per frequency spacing.

The derivative of $|C(t)|^2$ is the transition rate, Γ . Fig (3.1) can be used to find the transition rate. In Fig. (3.1), $g^2 = 0.5$ was used, which means that numerically, from the approximation given in Eq. (3.15), the transition rate is $\Gamma_{GR} = 2\pi g^2 = 1.57$. To find the transition rate from the numerical solution, a section of the plot early on in time when $|C(t)|^2$ is approximately linear is extracted. Take the derivative of this section by extracting data points, finding a curve fit, and taking the derivative of the curve fit. The resultant derivative is roughly constant, so the average will be the transition rate, Γ . The plot showing $|C(t)|^2$ versus time is plotted in Fig. (3.10)

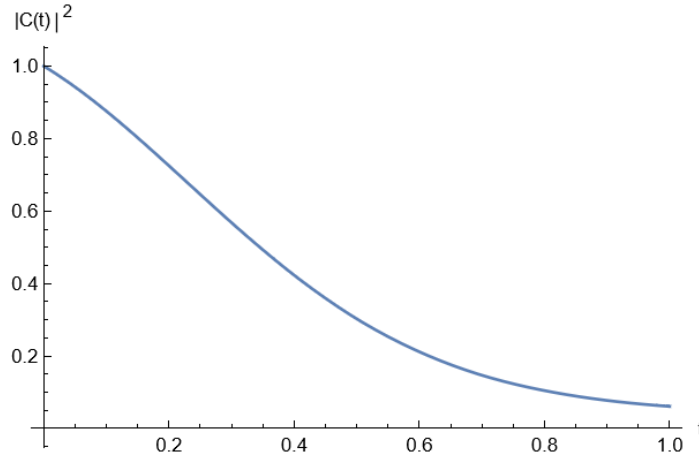


Figure 3.10: $|C(t)|^2$ for $N = 10$

Take the derivative of the function found to describe the probability amplitude, as shown in Fig. (3.10). The plot of the derivative yields a nearly constant value of approximately -1.6, which is recognized as $\pi/2$ and is the result calculated from Fermi's Golden Rule. The plot of $\frac{d}{dt}|C(t)|^2$ versus time is shown below.

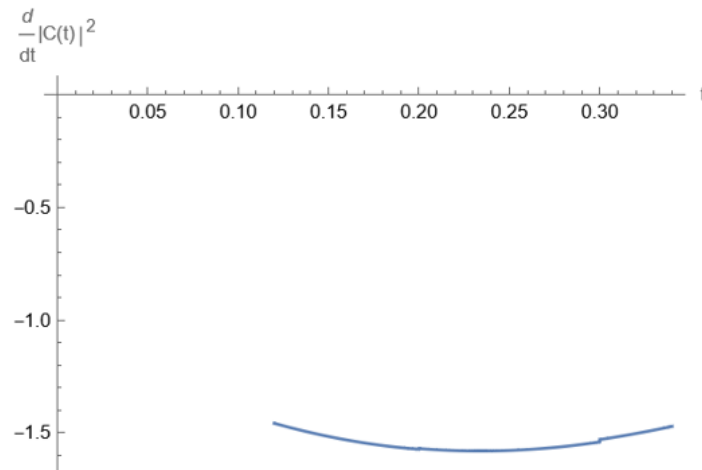


Figure 3.11: $\left|\frac{d}{dt}|C(t)|^2\right|$ versus time reveals the transition rate

Fig. (3.11) recovers the transition rate, Γ , and is consistent with Γ_{GR} from Fermi's Golden Rule. Note the transition rate recovered numerically is negative, which means the atom is leaving the $|c\rangle$ -state and entering the $|b\rangle$ -state.

CHAPTER 4

DENSITY MATRIX FOR THE $(N+1)$ -STATE MODEL

The density matrix is a mathematical representation of probabilities of quantum states. The density matrix contains sufficient information about the state of a particle that it could be used to represent the state of a particle instead of the wave function. It can be calculated for pure states using Eq. (4.1) [3].

$$\hat{\rho} = |\Psi\rangle \langle\Psi| \tag{4.1}$$

The density matrix for pure states obeys certain properties, given in Eqs. (4.2), (4.3), (4.4), and (4.5). It is idempotent, hermitian and its trace is 1.

$$\rho^2 = \rho \tag{4.2}$$

$$\rho^\dagger = \rho \tag{4.3}$$

$$\text{Tr}(\rho) = \sum_i \rho_{ii} = 1 \quad (4.4)$$

$$\langle | A | \rangle = \text{Tr}(\rho A) \quad (4.5)$$

When the system is in mixed states, the probability of each state is weighted. The system is said to be in mixed states for two types of situations. The first is due to ignorance about the system. For example, when an electron emerges from a particle accelerator, it could have spin up, spin down, or a linear combination of both spin up and spin down. This lack of knowledge about the state of the electron is not due to any scientific principle; there is merely ignorance about the state of the electron. In this case, the state of the particle would be described by the probability of each possible state $|\Psi_k\rangle$. These probabilities can be presented using the density matrix, as written in Eq. (4.6).

$$\hat{\rho} = \sum_k p_k |\Psi\rangle \langle\Psi| \quad (4.6)$$

Aside from ignorance, the density matrix for mixed states is useful to describe a subsystem. This arises when there is a system of entangled particles, wherein we cannot know the state of an individual particle in the system. This is separate from the mixed state instance of ignorance: it is not possible to know the subsystem precisely since it does not occupy a pure state [3].

In the context of my work, the density matrix of the particle can be calculated using Eq. (4.1) because the temperature is 0K and does not vary. In the future, when more research is done to study the dynamics of cold-atom sticking for varying temperatures, then the particle will occupy a mixed state and use Eq. (4.6). To describe my setup of the atom colliding with a membrane, I calculated the density matrix, as shown below.

$$\hat{\rho} = \begin{bmatrix} |C(t)|^2 & 0 \\ 0 & |B(t)|^2 \end{bmatrix} \quad (4.7)$$

Next, I can calculate the reduced density equation. This is given below.

$$\hat{\rho} = |C|^2 |c\rangle \langle c| + \sum_k |B_k|^2 |b\rangle \langle b| \quad (4.8)$$

The density matrix is useful for expressing the energy states of the particle. However, the main utility of the density matrix is to calculate the entanglement entropy. First, it is important to note the density matrix is diagonal, which provides mathematical convenience when calculating the entanglement entropy. The calculation for the entanglement entropy involves the log (base 2) of the density matrix. The log of a matrix is most simple to perform on a diagonal matrix, as the result is the natural log of each nonzero element. I will show the entanglement entropy calculation in the subsequent section.

CHAPTER 5

ENTANGLEMENT ENTROPY

Entanglement entropy (von Neumann entropy) is a quantitative way to describe the quantum entanglement within a system. In quantum mechanics, particles are said to be entangled when one particle affects characteristics of the other particle. It has applications in studying black holes that are interesting to cosmologists. I used the von Neumann definition of entanglement entropy, which is given in Eq. (5.1).

$$S(t) = -Tr(\hat{\rho}_A \ln \hat{\rho}_A) \tag{5.1}$$

Entropy is an essential measurement in thermodynamics. Entropy measures uncertainty in the state of a physical system [19]. Boltzmann and Gibbs entropies are two methods of calculating classical entropy. Entropy has useful applications to both classical physics and in the quantum regime.

A quantum mechanical system with density matrices $\hat{\rho}$ makes it useful to discuss the von Neumann entropy, which is an equation applicable to the quantum regime. Von Neumann entropy is given in Eq. (5.1). This definition of entropy has some similarities with Shannon entropy, a measure of entropy used in classical information

theory. Shannon entropy measures uncertainty associated with a classical probability distribution. Shannon entropy and von Neumann entropy agree under certain instances; if the states $|\psi_j\rangle$ are orthogonal, they agree. Otherwise, the von Neumann entropy is smaller than Shannon entropy [20].

The equation for von Neumann entropy can be rewritten such that λ_x are eigenvalues of the density matrix, ρ . In this instance, the Shannon entropy would be the case where $\lim_{x \rightarrow 0} x \log x = 0$.

$$S(\hat{\rho}) = - \sum_x \lambda_x \text{Log}_2 \lambda_x \quad (5.2)$$

The von Neumann entropy is used here to measure the quantum entanglement of the incident atom and the vibrations of a two-dimensional surface.

The result of the calculation is a time-dependent function $S(t)$ that can be plotted for each mode. As is evident from Eq. (5.1), the time-dependent entropy description is not a matrix, since it involves taking the negative trace of a matrix. The simplified result of the entanglement entropy is shown in Eq. (5.3).

$$S(t) = -|C(t)|^2 \text{Log}_2 |C(t)|^2 - \left(\sum_k |B_k|^2 \right) \text{Log}_2 \left(\sum_k |B_k|^2 \right) \quad (5.3)$$

Note the time in Eq. (5.3), is a rescaled time. It is time multiplied by a parameter, Ω_C which carries with it units of energy divided by \hbar .

As the entanglement entropy is a time dependent function, it will be effective to analyze the results on a plot versus time for both the single mode case and the multi-mode case. The entropy over long time periods is useful to determine the behavior of the particle. The outcome of the entropy is indicative of whether the particle stuck

to the surface. Eq. (5.4) shows the limit of $S(t)$ as time approaches infinity, where the lowercase s is the probability of sticking.

$$\lim_{t \rightarrow \infty} S(t) \rightarrow (1 - s) \text{Log}_2(1 - s) - s \text{Log}_2 s \quad (5.4)$$

5.1 SINGLE-MODE CASE

First, the entanglement entropy can be numerically calculated for the idealized case when there is no damping. Using the same conditions as that of Fig. (3.1), the von Neumann entropy, $S(t)$ is plotted versus time below, in Fig. (5.1).

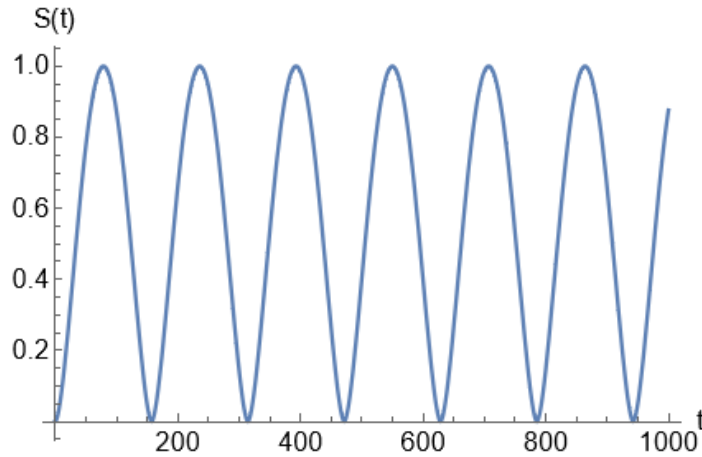


Figure 5.1: Entanglement Entropy for a single-mode with parameters $p = 0.01$ and $w = 1$

The entropy can similarly be shown for the off-resonance case below.

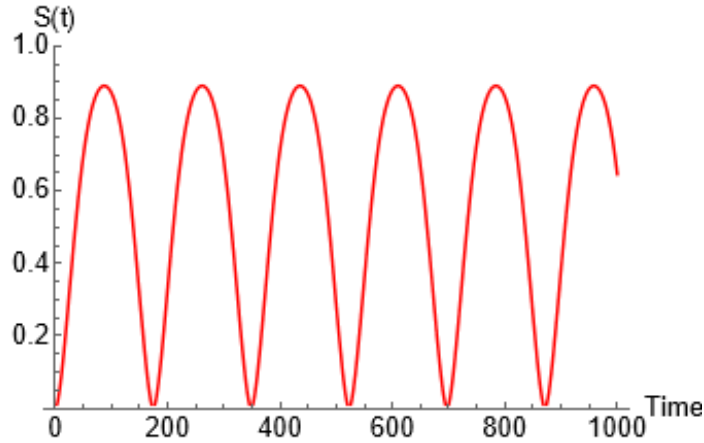


Figure 5.2: Entanglement Entropy for a single-mode with parameters $p = 0.01$ and $w = 0.97$

In Fig. (5.2), the plot is shown for parameters close to resonance. The same parameters were used in Fig. (3.2) as for Fig. (5.2).

Fig. (5.1) plots the entanglement entropy versus time for the single-mode case. If $S = 0$, the atom is either in the $|c\rangle$ -state or in the $|b\rangle$ -state with 1 vibron present. To determine the state of the atom, the entropy plot must be analyzed in conjunction with the plot of $|C(t)|^2$ as $\lim t \rightarrow \infty$. If the atom is determined to be in the $|c\rangle$ -state, then the width of the curve corresponds to the adsorption time, which can be calculated by finding the time it takes for entanglement entropy to return to a value sufficiently close to the initial von Neumann entropy.

To graph the entanglement entropy versus time in a manner that makes contact with experimental conditions, I input an imaginary part to the w parameter in the multimode case as follows. Having an imaginary part in one of the parameters is a better approximation of a situation that is feasible in the real world because the vibrations of the surface will damp.

5.2 MULTIMODE CASE

For 2 and 3 modes, the von Neumann entropy is graphed in Figs. (5.3) and (5.4) to model the von Neumann entropy versus time. For each different mode, there is a different frequency. For each mode that is added, the frequency spacing decreases.

The graphs in Fig. (5.3) and 5.4 are graphed over the same timescale.

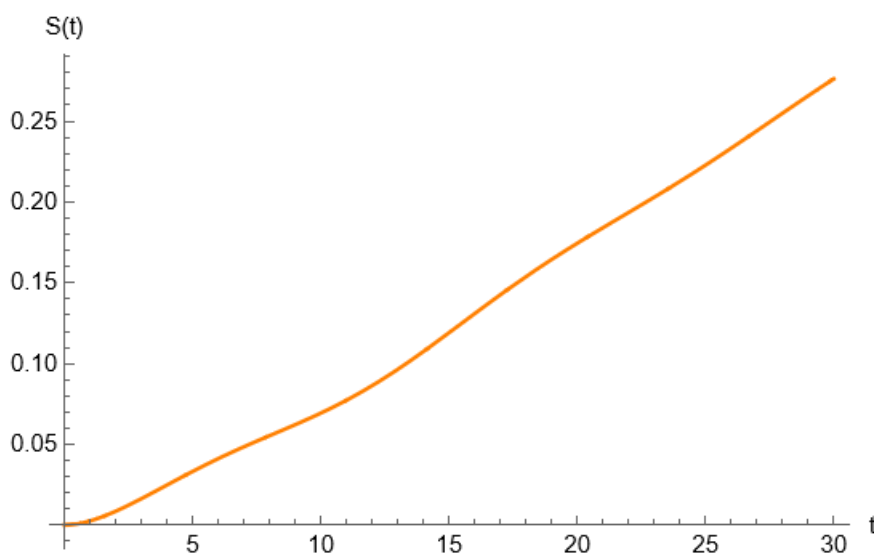


Figure 5.3: Entropy for 2 modes with parameters $p = 0.01$, $w_1 = 0.5 - i0.03$, $w_2 = 1 - i0.03$

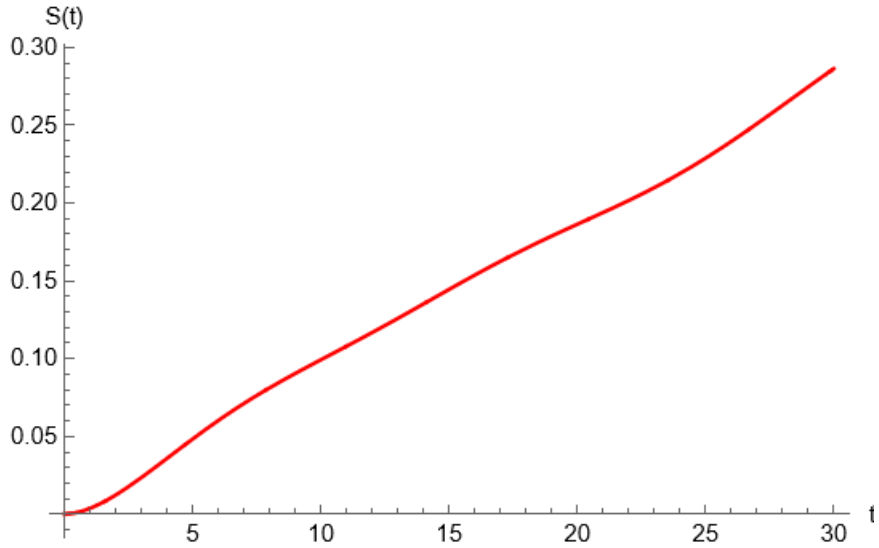


Figure 5.4: Entropy for 3 modes using parameters $p = 0.01$ and $w_1 = 0.5 - i0.03$, $w_2 = 0.75 - i0.03$, and $w_3 = 1 - i0.03$

Figs. (5.3) and (5.4) exhibit roughly a constant entropy rate.

Using the Laplace transform method and obtaining a numerical solution for $|C(t)|^2$, I can use the von Neumann equation for entropy to numerically calculate the entanglement entropy for $N = 10$. This plot is given in Fig. (5.5).

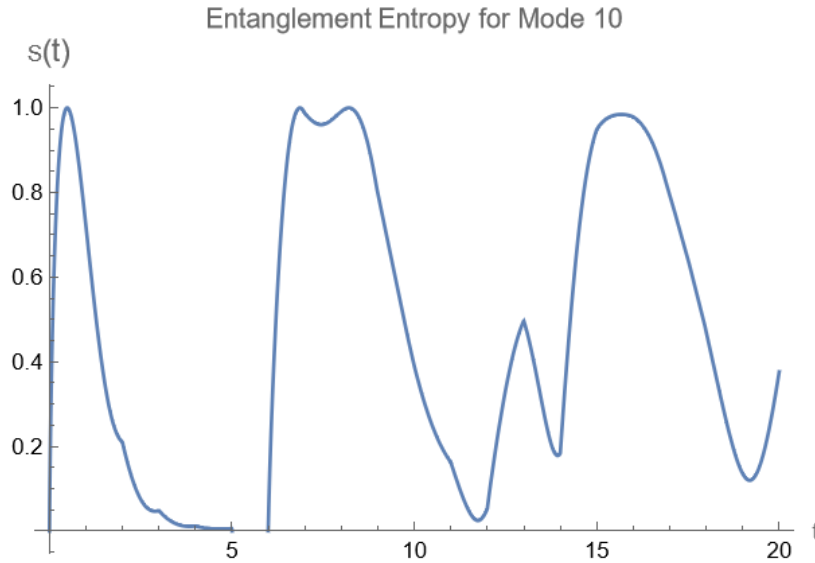


Figure 5.5: Entanglement Entropy for the $N=10$ Case with $g_0 = .5; b = 5$

The entanglement entropy plot over a relatively short timescale in the 10 mode case begins at an initial state $S(0) = 0$. In the model, since b is a real number with no imaginary part, there is no damping. Then, the entropy oscillates, with quantum revivals roughly occurring at each interval of 2π .

The same Laplace transform method can be applied to entropy when there is damping by using $b = 5 - i\frac{\pi}{6}$. Using this model to then find the entanglement entropy produces Fig. (5.6).

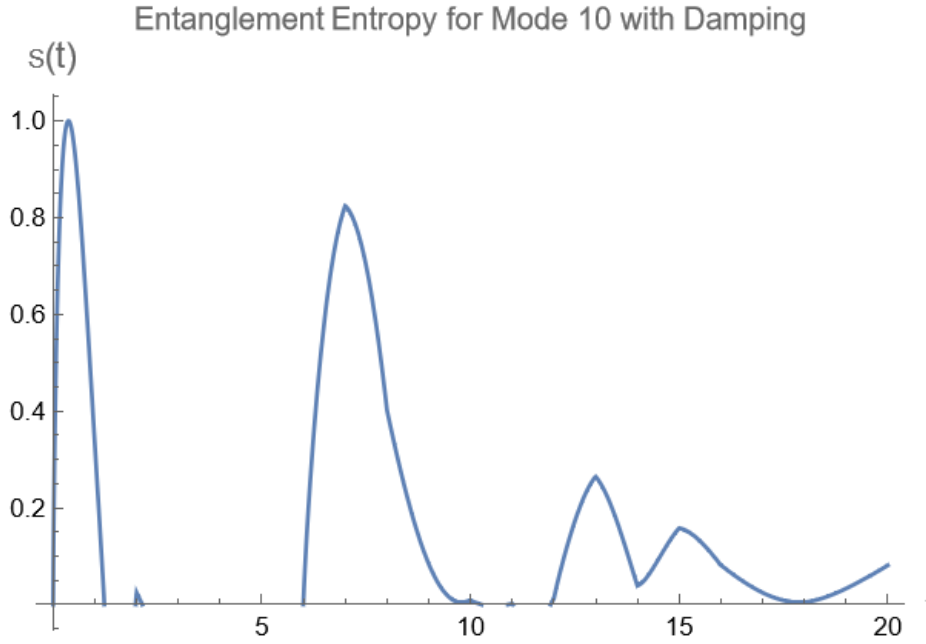


Figure 5.6: Entanglement Entropy for the $N=10$ case with $g_0 = .5; b = 5 - i\frac{\pi}{6}$

The entanglement when there is damping shows the atom transition to the bound state. As all other graphs of entropy, it begins at $S(0) = 0$. Then, an unstable entangled state is formed and decays into the bound state with a small number of vibrons that is close to 0. At intervals of 2π , there are quantum revivals as the atom return to the gas phase. The relative maxima of entropy damp over time.

Fig. (5.7) plots both $N = 10$ mode with damping and without damping, for comparison.

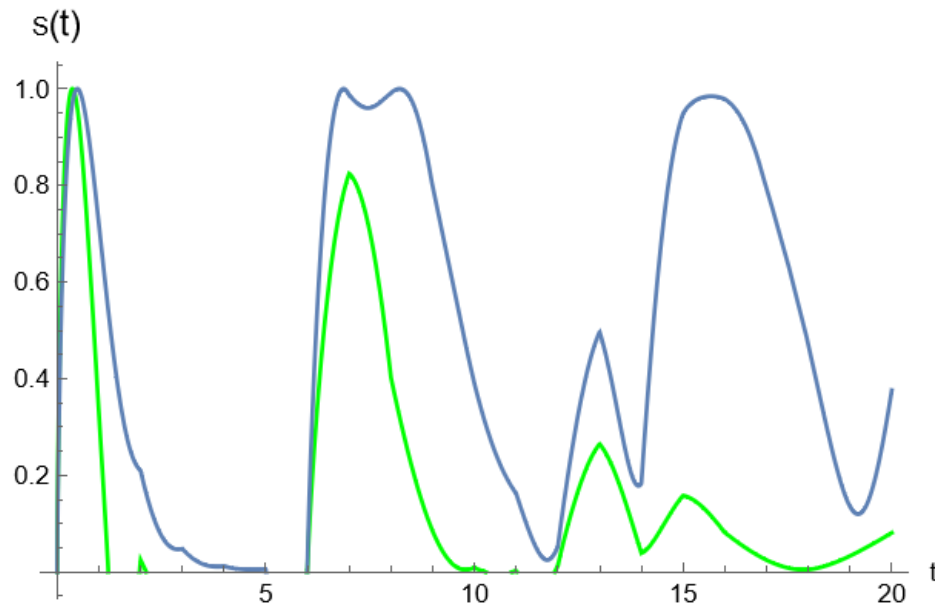


Figure 5.7: Entanglement Entropy for the $N = 10$ case with $g_0 = .5; b = 5 - i\frac{\pi}{6}$ in green and with $g_0 = .5; b = 5$ in blue

CHAPTER 6

CONCLUSIONS AND FUTURE WORK

This thesis describes the quantum sticking and entanglement entropy of a cold atom on a surface. A time-dependent ansatz for the system wave function derived coupled ODEs to describe the potential outcomes of the system, which were presented in Eqs. (2.7) and (2.8). Analytically solving these equations using methods of ODES revealed an analytical solution for the single-mode case to describe $C(t)$, which was given in Eq. (2.14).

In a physical system, the vibrons have a finite lifetime. This scenario was modeled by adding a small imaginary component to the frequency. Plotting numerical solutions with an imaginary part showed the oscillations of the transition probability damp over time.

From numerical solutions to $C(t)$ and $B_n(t)$, the entanglement entropy was determined. The time-dependent entanglement entropy (von Neumann entropy), $S(t)$, was plotted versus time for the single-mode case and for the multi-mode case. The entropy begins at zero, grows to a local maximum, and then returns to zero. Later throughout time, there is a “quantum revival” where the entanglement entropy grows to a local maximum and subsequently collapses to zero.

The investigation of the entanglement entropy and quantum sticking of a cold

atom remains with some further questions that could be a future line of inquiry. This thesis only covered the condition for where the temperature is 0K. To create a more complete study of quantum sticking and entanglement entropy, the case of non-zero temperature should be studied. We would like to see how temperature would affect the adsorption and entanglement entropy. The temperature would have to stay cold and close to absolute zero to remain a low-energy interaction. It would be useful to investigate the range of 0-20K.

Varying the temperature would necessitate different methods. The density matrix invokes the pure state formula when the temperature is 0K. When the temperature is nonzero, the density matrix would require the mixed state formula to calculate. Further, the time-dependent ansatz would need to be modified to include thermal effects. This could be done by using the time-dependent variational method of Dirac and Frenkel [6] [7].

APPENDIX: MATHEMATICA CODE

```
ClearAll[p, w, time];
p = 0.1; w = 0.05 - 0.03 i;
time = 15000;

solution1mode =
  NDSolve[{I c'[t] == c[t] + p b1[t], I b1'[t] == w b1[t] + p c[t],
    b1[0] == 0, c[0] == 1}, {c, b1}, {t, 0, time}]

Plot[{Abs[c[t] /. solution1mode]^2}, {t, 0, time},
  PlotStyle -> Red, PlotLabel -> "Single Mode Damped Oscillations",
  AxesLabel -> {"Time", "|C(t)|^2"}]

rho = {{Abs[c[t] /. solution1mode]^2, 0},
  {0, Abs[b1[t] /. solution1mode]^2}}

S1[t_] :=
  -Abs[c[t] /. solution1mode]^2 *
  (Log2[Abs[c[t] /. solution1mode]^2]) -
  Abs[b1[t] /. solution1mode]^2 * Log2[Abs[b1[t] /. solution1mode]^2]

entropymodel = Plot[{Re[S1[t]]}, {t, 0, time}, PlotRange -> All,
  PlotStyle -> Red]
```

Figure 6.1: Mathematica code to numerically solve for $C(t)$ and $B(t)$, then find density matrix, ρ and the entanglement entropy, $S1(t)$.

ACKNOWLEDGMENTS

I would like to thank my advisor, Dr. Dennis Clougherty, for teaching me at least half of the physics I know and for his guidance in undertaking this research.

Thank you to Dr. Valeri Kotov and Dr. Francois Dorais for graciously being part of my thesis committee.

Thank you to the physics community at UVM, and thank you to everyone who has supported me throughout my time at the University of Vermont.

BIBLIOGRAPHY

- [1] von Neumann, J. *Mathematical Foundations of Quantum Mechanics* (Princeton University Press, Princeton, NJ, 1955).
- [2] Mereghetti, E. Electric dipole moments: a theory overview (2018). **1810.01320**.
- [3] Griffiths, D. J. & Schroeter, D. F. *Introduction to Quantum Mechanics* (Cambridge University Press, England, 2018).
- [4] Nichols, N. S., Maestro, A. D., Wexler, C. & Kotov, V. N. Adsorption by design: Tuning atom-graphene van der waals interactions via mechanical strain. *Physical Review B* **93** (2016). URL <https://doi.org/10.1103/PhysRevB.93.205412>.
- [5] Lennard-Jones, J. E. Perturbation problems in quantum mechanics. *Proceedings of the Royal Society A* **129**, 598–615 (1930).
- [6] Dirac, P. Note on exchange phenomena in the thomas atom. *Mathematical Proceedings of the Cambridge Philosophical Society* **26**, 376–385 (1930).
- [7] Frenkel, J. Wave mechanics: Advanced general theory. *The Mathematical Gazette* **18**, 208–209 (1934).
- [8] Cornell, E. A. & Wieman, C. E. The bose-einstein condensate. *Scientific American* **26** (1998). URL <https://www.scientificamerican.com/article/bose-einstein-condensate/>.
- [9] The nobel prize in physics 2001. URL <https://www.nobelprize.org/prizes/physics/2001/popular-information/>.
- [10] The nobel prize in physics 1997. URL <https://www.nobelprize.org/prizes/physics/1997/press-release/>.

- [11] Garcia-Sanchez, D. *et al.* Imaging mechanical vibrations in suspended graphene sheets. *Nano Letters* **8**, 1399–1403 (2008). URL <https://doi.org/10.1021/nl080201h>. PMID: 18402478, <https://doi.org/10.1021/nl080201h>.
- [12] Bunch, J. S. *et al.* Impermeable atomic membranes from graphene sheets. *Nano Letters* **8**, 2458–2462 (2008). URL <https://doi.org/10.1021/nl801457b>. PMID: 18630972, <https://doi.org/10.1021/nl801457b>.
- [13] Clougherty, D. P. Quantum sticking of atoms on membranes. *Physical Review* **90** (2014).
- [14] Clougherty, D. P. & Kohn, W. Low energy behavior of quantum adsorption (1992). [cond-mat/9205004](https://arxiv.org/abs/cond-mat/9205004).
- [15] Sengupta, S. & Clougherty, D. P. Infrared problem in cold atom quantum physisorption on 2d materials. *Journal of Physics: Conference Series* **1148**, 012007 (2018). URL <https://dx.doi.org/10.1088/1742-6596/1148/1/012007>.
- [16] Merlin, R. Rabi oscillations, floquet states, fermi’s golden rule, and all that: Insights from an exactly solvable two-level model. *American Journal of Physics* **89**, 26–34 (2021). URL <https://doi.org/10.1119/10.0001897>. <https://doi.org/10.1119/10.0001897>.
- [17] Sakurai, J. J. & Napolitano, J. *Modern Quantum Mechanics* (Cambridge University Press, 2020), 3 edn.
- [18] Zhang, J. M. & Liu, Y. Fermi’s golden rule: its derivation and breakdown by an ideal model. *European Journal of Physics* **37**, 065406 (2016). URL <https://doi.org/10.1088/2F0143-0807/2F37/2F6/2F065406>.
- [19] Michael A. Nielsen, I. L. C. *Quantum Computation And Quantum Information 10th Anniversary Edition* (Cambridge University Press, Cambridge, England, 2012).
- [20] Pathria, R. & Beale, P. D. *Statistical Mechanics* (Academic Press, Cambridge, Massachusetts, 2022).